32. G. I. Vladimer *et al.*, The NLRP12 Inflammasome Recognizes Yersinia pestis. *Immunity*. **37**, 96–107 (2012).

33. W. J. Kaiser *et al.*, RIP3 mediates the embryonic lethality of caspase-8-deficient mice. *Nature*. **471**, 368–372 (2011).

34. L. Salmena *et al.*, Essential role for caspase 8 in T-cell homeostasis and T-cell-mediated immunity. *Genes Dev.* **17**, 883–895 (2003).

35. K. Newton, X. Sun, V. M. Dixit, Kinase RIP3 is dispensable for normal NF-kappa Bs, signaling by the B-cell and T-cell receptors, tumor necrosis factor receptor 1, and Toll-like receptors 2 and 4. *Mol. Cell. Biol.* **24**, 1464–1469 (2004).

36. A. Polykratis *et al.*, Cutting Edge: RIPK1 Kinase Inactive Mice Are Viable and Protected from TNF-Induced Necroptosis In Vivo. *J. Immunol.* **193**, 1539–1543 (2014).

37. S. B. Berger *et al.*, Cutting Edge: RIP1 Kinase Activity Is Dispensable for Normal Development but Is a Key Regulator of Inflammation in SHARPIN-Deficient Mice. *J Immunol*. **192**, 5476–5480 (2014).

38. J. M. Murphy *et al.*, The pseudokinase MLKL mediates necroptosis via a molecular switch mechanism. *Immunity*. **39**, 443–453 (2013).

39. S. W. Montminy *et al.*, Virulence factors of Yersinia pestis are overcome by a strong lipopolysaccharide response. *Nat Immunol*. **7**, 1066–1073 (2006).

40. S. B. Berger *et al.*, Characterization of GSK ′963 : a structurally distinct , potent and selective inhibitor of RIP1 kinase. *Cell Death Discov.* **1** (2015), doi:10.1038/cddiscovery.2015.9.

41. W. J. Kaiser *et al.*, Toll-like receptor 3-mediated necrosis via TRIF, RIP3, and MLKL. *J. Biol. Chem.* **288**, 31268–31279 (2013).

42. Y. Dondelinger *et al.*, MK2 phosphorylation of RIPK1 regulates TNF-mediated cell death. *Nat. Cell Biol.* **19**, 1237–1247 (2017).

43. J.-B. Denault, G. S. Salvesen, Expression, purification, and characterization of caspases. *Curr. Protoc. Protein Sci.* **30** (2003).

44. M. L. Gonzalez Ramirez *et al.*, Extensive peptide and natural protein substrate screens reveal that mouse caspase-11 has much narrower substrate specificity than caspase-1. *J. Biol. Chem.* **293**, 7058–7067 (2018).

45. D. Ratner *et al.*, Manipulation of Interleukin-1β and Interleukin-18 Production by Yersinia

pestis Effectors YopJ and YopM and Redundant Impact on Virulence. *J. Biol. Chem.* **291**, 9894–9905 (2016).

46. L. W. Peterson *et al.*, RIPK1-dependent apoptosis bypasses pathogen blockade of innate signaling to promote immune defense. *J. Exp. Med*. **214**, 3171–3182 (2017).

47. S. Michel, S. Falkow, Invasin Expression in Yersinia pseudotuberculosis. *Infect. Immun.* **60**, 4414–4417 (1992).

48. Y. Zhang, J. B. Bliska, YopJ-Promoted Cytotoxicity and Systemic Colonization Are Associated with High Levels of Murine Interleukin-18, Gamma Interferon, and Neutrophils in a Live Vaccine Model of Yersinia pseudotuberculosis Infection. *Infect. Immun.* **78**, 2329–2341 (2010).

49. G. Denecker *et al.*, Effect of Low- and High-Virulence Yersinia enterocolitica Strains on the Inflammatory Response of Human Umbilical Vein Endothelial Cells. *Infect. Immun.* **70**, 3510–3520 (2002).

50. J. Ruan, S. Xia, X. Liu, J. Lieberman, H. Wu, Cryo-EM structure of the gasdermin A3 membrane pore. *Nature*. **557** (2018).

51. D. Boucher *et al.*, Caspase-1 self-cleavage is an intrinsic mechanism to terminate inflammasome activity. *J. Exp. Med.* **215**, 827–840 (2018).

52. K. W. Chen *et al.*, Noncanonical inflammasome signaling elicits gasdermin D–dependent neutrophil extracellular traps. *Sci. Immunol.* **3**, eaar6676 (2018).

53. V. A. K. Rathinam *et al.*, TRIF licenses caspase-11-dependent NLRP3 inflammasome activation by gram-negative bacteria. *Cell*. **150**, 606–619 (2012).

54. R. J. Platt *et al.*, CRISPR-Cas9 knockin mice for genome editing and cancer modeling.

Cell. **159**, 440–455 (2014).

55. O. Shalem *et al.*, Genome-Scale CRISPR-Cas9 Knockout Screening in Human Cells. *Nat. Biotechnol.* **31**, 827–32 (2013).

56. J. G. Doench *et al.*, Rational design of highly active sgRNAs for CRISPR-Cas9–mediated gene inactivation. *Nat. Biotechnol.* **32**, 1262–7 (2014).

Science
AAAS

Supplementary Materials for

Pathogen blockade of TAK1 triggers caspase-8 dependent cleavage of Gasdermin D and cell death

Pontus Orning, Dan Weng, Kristian Starheim, Dmitry Ratner, Zachary Best, Bettina Lee, Alexandria Brooks, Shiyu Xia, Hao Wu, Michelle A. Kelliher, Scott B. Berger, Peter J. Gough, John J. Bertin, Megan M. Proulx, Jon D. Goguen, Nobuhiko Kayagaki, Katherine A. Fitzgerald and Egil Lien*

*To whom correspondence should be addressed. E-mail: Egil.Lien@umassmed.edu

This PDF file includes:

Materials and Methods

Mice

All experiments involving mice were approved by the Institutional Animal Care and Use Committee. Most mouse strains used in this study were described previously (*12*, *28*, *32*) and bred in-house. Caspase-8 KO mice are embryonically lethal, as caspase-8 is an inhibitor of RIPK3 mediated necroptosis (*33*). Caspase-$8^{-/-}$ $RIPK3^{-/-}$dKO mice (*33*) are viable and were originally bred by W. Kaiser and E. Mocarski from a caspase-$8^{-/+}$ allele generated by R. Hakem (Univ. of Toronto) (*34*) and RIPK3 KO (*35*) generated by K. Newton and V. Dixit (Genentech), and provided by Drs. Kaiser and Mocarski and C. Dillon and D. Green. $GSDMD^{-/-}$ mice (*7*) and $GSDMD^{D276A/D276A}$ knock-in cleavage dead mice (*29*) were generated at Genentech by V. Dixit, B. Lee and N. Kayagaki. RIPK1 D138N mutant mice (*36*) and $TNFR1^{-/-}$ mice (originally from Jackson Labs) were from M. Kelliher. RIPK1 kinase-dead K45A mutant mice (*37*) were generated at GSK and provided by J. Bertin. MLKL KO were provided by F. Chan and originally from W. Alexander (WEHI) (*38*). BMDMs were differentiated from bone marrow harvested from femurs and tibia of 6–20 week old mice.

Antibodies and reagents

Antibodies used in this study include mouse caspase-1 (#AG-20B-0042-C100, Adipogen), mouse ASC (sc-22514-R, Santa Cruz), mouse GSDMD (17G2G9, Genentech) (*6*), mouse IL1β (AF-401-NA, R&D), mouse cleaved caspase-8 (D5B2, Cell Signaling Technology, CST) mouse full length caspase-8 (1C12, CST), mouse cleaved caspase-3 (5A1E, CST), mouse caspase-7 (D2Q3L, CST) and actin (AC15, Novus Biologicals). Reagents used in this study include Pam3CSK4 (Invivogen), repurified TLR2 ligand-free LPS (E. coli O111:B4) (*39*), R848 (Invivogen), mouse TNF (Peprotech), RIPK1 inhibitor (GSK'963, GlaxoSmithKline) (*12*, *40*), RIPK3 inhibitor (GSK'872, GlaxoSmithKline) (*41*), pan-caspase inhibitor zVAD-fmk (62-761-01MG, Millipore), TAK1 inhibitor (TAK1-i) 5z-7-oxozeaneol (abbreviated to 5z7, 499610-1mg, EMD), TAK1 inhibitor NG25 (5429, Tocris Bioscience), MAPK p38 inhibitor (SB203580 Tocris Bioscience), IKK inhibitor (TPCA-1, 25-591-0, Tocris Bioscience) (*42*), ATP (Sigma Aldrich), and Nigericin (Invivogen). Inhibition and deletion of TAK1 (*20*) or IKKβ (*24, 43*) have been associated with IL-1β release and NLRP3 inflammasome activity. Recombinant active mouse caspase-1 (Cat no. 1181) and mouse caspase-8 (Cat no. 1188,) were from BioVision. Activity is given as 5000 U/mg (1 U/25 µl ~ 130 nM, we used 1 and 5 U per reaction) for caspase-8 when tested on peptide substrate by manufacturer, and for caspase-1, >3000 U/mg (1 U/25 µl > 270 nM, we used 1 U per reaction). Recombinant active human caspase-3 and caspase-8 (we used 100 and 500 nM, or 500 nM of each when combined) were from G. Salvesen, S. Snipas and the Salvesen lab (*44*, *45*). PI dye used for kinetic cell death measurements was purchased from Thermo Fisher (P1304MP), Hoechst from Thermo Fisher (62249), and EthD-1 from Sigma (46043). DSS crosslinker used for ASC oligomerization assays was purchased from Thermo Fisher (21658). For LDH assay we used the CytoTox 96 kit, (Promega G1780), for caspase-8 activity, we used Caspase-8 Glo (Promega G8200), and for ELISA we used IL-1β and IL-18 kits from R&D Systems.

Cell stimulations

Bone marrow derived macrophages (BMDMs) were differentiated in DMEM supplemented with 10% fetal calf serum (FCS), 25 mM HEPES, 5 µg/mL ciprofloxacin, and 10% L929

conditioned medium containing M-CSF for 6 days, essentially as described (*28*, *46*). Cells were stimulated with bacterial strains as described below, or with the chemical inhibitors 5z7 TAK1-i (0.4 μM), NG25 (5 μM), TPCA-1 IKK-i (5 μM), SB203580 MAPK p38-i (7 μM), GSK'963 RIPK1-i (1 μM), GSK'872 RIPK3-i (3 μM), and zVAD pan-caspase-inhibitor (25 μM). 5z7 was used in all experiments as TAK1-i. In the experiment shown in Fig S1C, 5z7 was compared to NG25, another TAK1 inhibitor. The relevant pathways were activated by simultaneous addition of TAK1-inhibitors and other stimuli (LPS, TNF, Pam3Cys, R848, bacteria). For GSK'963, GSK'872, and zVAD, these inhibitors were added 1 h before addition of subsequent stimuli. For stimulation with nigericin and ATP, cells were primed with 100 ng/ml LPS for 3 hours before stimulation. All IL-1β experiments were performed for 5 h of stimulation unless otherwise stated.

Bacterial strains and growth conditions

The pgm-deficient but type III secretion system pCD1+ strain of *Y. pestis* (KIM5) as well as its mutant derivatives (ΔYopJ) were earlier described (*32*, *39*). The *Y. pseudotuberculosis* IP32777 (serogroup O:1, also known as IP2777) and IP32777ΔYopJ (*47–49*), were provided by I. Brodsky and J. Bliska. *Y. enterocolitica* A127/90 (serogroup O:8 biotype IA – a wild-type, virulent strain) and A127/90 ΔYopP (called YopJ in *Y. pestis* and *Y. pseudotuberculosis*) were provided by R. Adkins and G. Cornelis (*50*) *Y. pestis* strains were grown in tryptose-beef extract broth with 2.5 mM $CaCl_2$ and *Y. pseudotuberculosis* strains were grown in 2xYT broth. *Y. enterocolitica* strains were grown in LB broth. All *Yersinia* strains were plated overnight from frozen glycerol stocks and then grown at 26°C in liquid broth overnight; on the day of infection cultures were diluted 1:10 and grown for 1 hour at 26°C followed by a shift to 37°C for 2 hours. This transition mimics bacterial conditions that can be observed during transmission from fleas to their mammalian hosts and is important to up-regulate expression of the T3SS and allowing for the presence of some TLR4-activating LPS, while minimizing expression of F1 protein capsule (*12*). Bacteria were then washed three times in PBS, quantified by OD600, and added to cells at a multiplicity of infection (MOI) of 10 (*Y. pestis*, *Y. enterocolitica*) or 40 (*Y. pseudotuberculosis*) CFU per cell. *Salmonella enterica* serovar Typhimurium strain SL1344 (provided by M. O'Riordan) bacteria were grown in LB medium similarly to *Yersinia* strains but at 37°C. *Salmonella* bacteria were added to cells at MOI 2. Gentamicin (50 μg/ml) was added to cultures 2 h post infection to limit extracellular replication of *Yersinia* and *Salmonella* bacteria, with the exception of experiments shown in Fig 4E, G.

Cell death assays

The LDH assay was used to measure cell death at a 4-h end point, unless otherwise stated in the figure. For this assay, the medium was replaced with X-vivo (Lonza) supplemented with 3.5% FCS and 25 mM HEPES prior to infection. Additionally, a kinetic cell death assay using a DNA binding dye was performed as follows. The cells were incubated with 2 μM ethidium homodimer (EthD-1, Sigma catalog no. 46043) in the DMEM medium mentioned above 1 h before adding bacteria, essentially as described (*46*). Upon infection, the plate was placed in a Synergy H4 plate reader at 37°C, and fluorescence measurements were made every 10 min at excitation: 530 nm, emission: 645 nm. Increased fluorescence correlates with DNA binding by EthD-1 upon entry through increasingly permeable cell membranes as cell death progresses. We also used the Biotek kinetic cell death reader Cytation3 to measure PI positive cells over time during infection, and collect bright field images (Fig S6G, H).

Immunoprecipitations and immunoblots

Cells were infected at MOI 10 for *Yersinia* or MOI 2 for *Salmonella* as described above, and harvested at different timepoints post infection with 50 μg/mL gentamicin added after 2 hours. For IP, cells were washed once and lysed in IP buffer for 15 minutes (1% Triton X-100, 150 mM NaCl, 5 mM KCl, 2 mM $MgCl_2$, 1 mM EDTA, 25 mM Tris-HCl, pH 7.4) with protease and phosphatase inhibitor (#04693116001 and #04906845001, Roche). Lysates was cleared by centrifugation at 16,000 g and a fraction was saved as loading input control. The remaining lysate was cleared once with protein A agarose beads (Thermo #20398) to remove non-specific protein binding, followed by incubation with fresh beads and pull-down antibody against caspase-8 or GSDMD over night at 4°C. Beads were then washed 5-7 times in IP buffer, and bound proteins were eluted by direct addition of SDS loading buffer with 2 mM DTT. Beads and saved lysate were analyzed by immunoblot. For caspase-1 and caspase-8 immunoblot, a combined cell lysate and supernatant was loaded on the gel. For GSDMD blots only the cell lysate was loaded on the gel.

GSDMD cleavage assay

Recombinant mouse GSDMD was generated similarly as described previously for human GSDMD (*51*). Briefly, full-length mouse GSDMD sequence was cloned into the pDB.His.MBP vector to append a tobacco etch virus (TEV)-cleavable N-terminal His_6-MBP tag. *E. coli* BL21 (DE3) cells were transformed with the vector and grown at 18°C overnight in LB medium supplemented with 50 μg/ml kanamycin. Expression was induced with 0.5 mM isopropyl-β-D-thiogalactopyranoside (IPTG) after OD_{600} reached 0.8. Harvested cells were lysed in a buffer containing 25 mM Tris-HCl pH 8.0, 150 mM NaCl, 5 mM imidazole. The lysate was clarified by centrifugation and the supernatant was incubated with Ni-NTA resin (Qiagen) for 1 h at 4°C. The recombinant protein was eluted using the lysis buffer supplemented with 100 mM imidazole. The His_6-MBP tag was removed by overnight TEV cleavage at 4°C, after which mouse GSDMD was further purified by ion exchange and size exclusion using HiTrap Q and Superdex 200 columns (GE Healthcare Life Sciences), respectively. For cleavage of purified mouse GSDMD by caspase-8, we performed immunoprecipitation (IP) on LPS+5z7 treated immortalized $Gsdmd^{-/-}$ BMDMs using cleaved caspase-8 antibody for 16 h. The IP lysates were then washed 5-7 times, and resuspended in protein cleavage buffer (50mM HEPES pH 7.5, 3mM EDTA, 150mM NaCl, 0.005% (vol/vol) Tween-20 and 10 mM DTT). Recombinant mouse GSDMD (2 μg) was added and samples were incubated at 37°C for 1 h. Cleavage of GSDMD was examined by immunoblot as previously described. Cleavage of recombinant GSDMD with recombinant caspases was done in a 25 μl volume with the indicated concentrations of caspases and 2 μg of GSDMD in the cleavage buffer mentioned above. It should however be noted that direct comparisons of caspase activities and cleavage efficiencies towards substrates can be difficult due to different sources of reagents, variations in specific activities and purification processes. In addition, recombinant preparations may contain different molecular species, and the specific isoforms responsible for cleavage may not be as previously thought, such as for caspase-1 (*52*). Caspase activity given in units (U) is typically measured towards synthetic substrates containing cleavage site tetrapeptides, however, other protein features different from the tetrapeptide may also impact caspase cleavage of actual protein substrates (*45*). The ideal comparisons may be between

proteins/caspases that are produced in similar processes, and over a range of concentrations (*53*), to determine k_{cat}/K_m values (*45*).

ASC oligomerization

Cross-linking assays of speckling ASC proteins were performed as previously described (*54*). Briefly, cells were infected with bacteria or LPS+5z7 before being harvested, washed, and lysed in NP-40 lysis buffer. Cell debris was removed and the remaining supernatant was centrifuged at a high rpm to separate big protein complexes. The lysate was saved for input control, and the pellet was washed in CHAPS buffer (0.1% CHAPS, 150 mM KCl, and 50 mM HEPES pH 7.4) and cross-linked with DSS. Both fractions were then added SDS loading buffer and analyzed by immunoblot. Typically, productive stimulation will result in pelleting of inflammasome aggregates and subsequent cross-binding of ASC containing complexes, and enable visualization of monomers as well as dimers and higher order structures on the immunoblot. In contrast, absence of stimulation will result in a failure to visualize both monomers and higher order structures. Soluble ASC in lysates was also analyzed as controls, however, this detection is often reduced in conditions of high cell death with longer incubations, likely due to leakage of ASC from cells via membrane pores and ruptures. Band density of higher order ASC complexes (dimers and higher) were scanned by ImageJ and displayed as % of WT stimulation (Table S2).

CRISPR

CRISPR/Cas9 C57BL/6 BMDMs endogenously expressing Cas9 (*55*) were immortalized with J2 retrovirus expressing c-myc and c-raf. Cells were transduced with lentivirus containing lentiGuide-Puro cloned with sgRNA using the F. Zhang protocol (*56*). sgRNA sequences were chosen using the Doench algorithm (*57*) and the online web tool Benchling.

Statistical analysis

In vitro assays were analyzed by unpaired two-tailed *t*-tests for two groups, or one-way ANOVA followed by Bonferroni post-test for three groups or more. For kinetic cell death assays, area under the curve (AUC) was calculated for each sample and one-way ANOVA followed by Bonferroni post-test was performed to determine significance. Values where $p<0.05$ were considered significant.

Ethics statement

All animal studies were performed in compliance with the federal regulations set forth in the Animal Welfare Act (AWA), the recommendations in the Guide for the Care and Use of Laboratory Animals of the National Institutes of Health, and the guidelines of the UMass Medical School Institutional Animal Use and Care Committee. All protocols used in this study were approved by the Institutional Animal Care and Use Committee at the UMass Medical School (protocols A-2332 and A-2339).

Supplementary Figure 1.

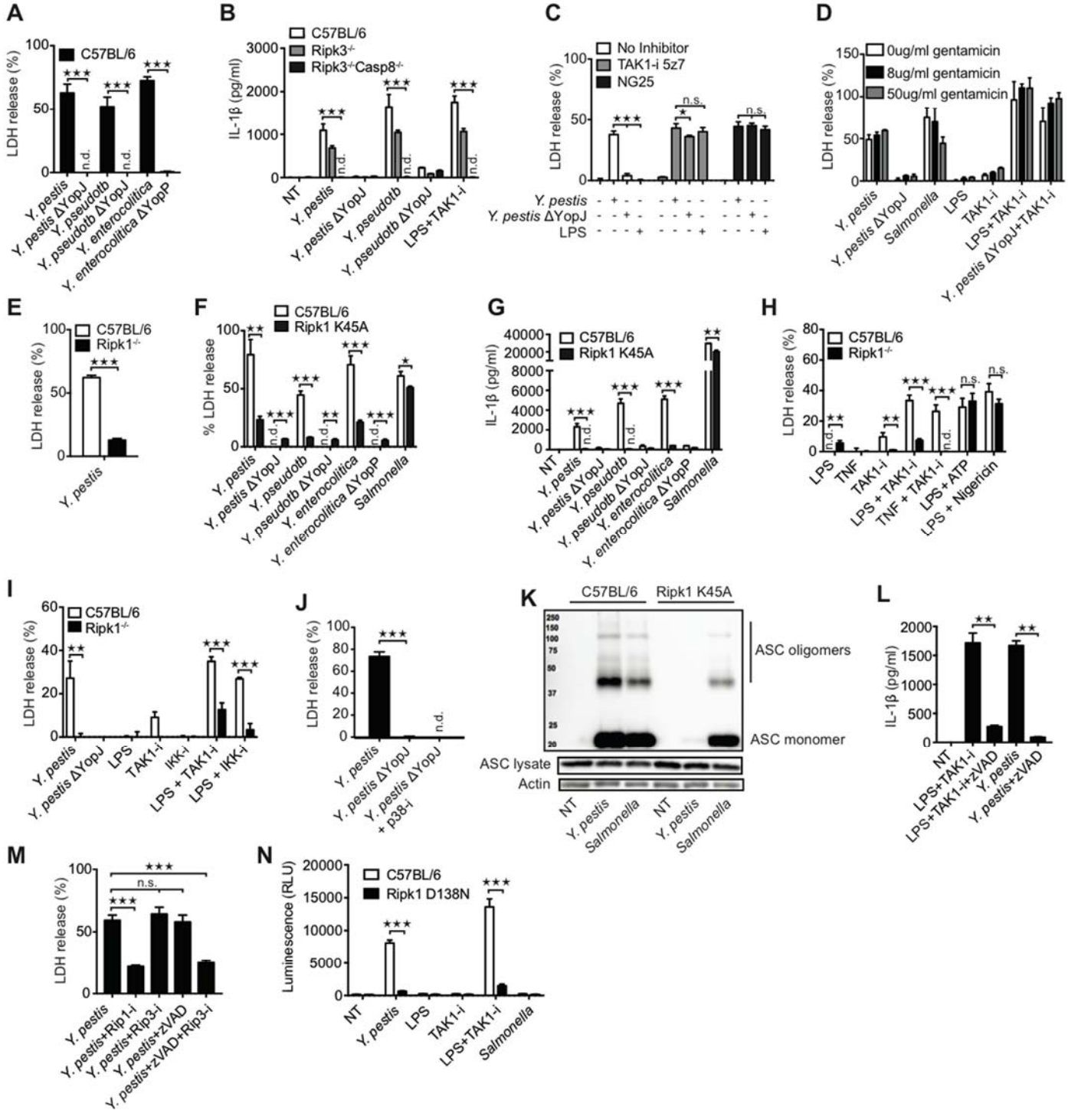

Fig. S1. Bacterial or small molecule inhibition of TAK1 or IKK triggers cell death, IL-1β release, and ASC oligomerization. (**A**) LDH release in C57BL/6 BMDMs challenged with *Y. pestis*, *Y. pseudotuberculosis*, or *Y. enterocolitica* or the equivalent strains lacking the effector protein YopJ or YopP. (**B**) IL-1β release from the indicated genotypes infected with *Y. pestis*, *Y. pseudotuberculosis*, or *S.* Typhimurium, or treated with LPS (100 ng/ml) and the TAK1 inhibitor 5Z-7-Oxozeaenol (TAK1-i, 5z7, 0.4 μM). (**C**) LDH release from C57BL/6 macrophages after inhibition of TAK1 with 5z7 TAK1-i (0.4 μM) or NG25 (5 μM) in the absence or presence of LPS (100 ng/ml), *Y. pestis* or *Y. pestis* ΔYopJ. (**D**) Increasing doses of gentamicin minimally affect cell death (measured by LDH) induced in C57Bl/6 BMDM after 3 h infection with *Y. pestis*. (**E-I**) LDH release from C57BL/6 or Ripk1$^{-/-}$ fetal liver macrophages (FLM) or BMDM from C57Bl/6 or RIPK1 K45A after challenge with *Y. pestis*, or TNF (50 ng/ml) and LPS (100 ng/ml) in the presence or absence of TAK1 inhibition (5z7 0.4 μM) or IKK inhibition (TPCA-1 5 μM**)**. Some cells were challenged with *Y. pestis*, *Y. pseudotuberculosis*, or *Y. enterocolitica* or the equivalent strains lacking the effector protein YopJ (or YopP in *Y. enterocolitica*). LDH and IL-1β release was measured after 3 h and 5 h respectively. (**J**) C57BL/6 BMDMs were challenged with *Y. pestis* and *Y. pestis* ΔYopJ in the presence or absence of MAPK p38 inhibitor (p38-i) SB203580. (**K**) BMDMs from the indicated genotypes were infected with *Y. pestis* or *Salmonella* and analyzed by immunoblotting for oligomerization of ASC in the inflammasome-enriched and cross-linked lysates. (**L**-**M**) C57BL/6 BMDMs were pretreated for 1 h with the pan-caspase inhibitor zVAD-fmk (25 μM), RIPK1 inhibitor GSK'963 (1 μM), or RIPK3 inhibitor GSK'872 (3 μM) before challenged with *Y. pestis* or treated with LPS+5z7. Cells were analyzed for LDH release (**M**) after 3 h, and IL-1β release (**L**) after 5 h. (**N**) C57BL/6 and Ripk1 D138N BMDMs were challenged with *Y. pestis*, LPS, TAK1-i, LPS+TAK1-i, or *S.* Typhimurium for 5 h and caspase-8 enzymatic activity was analyzed by caspase-8 Glo assay. Activity was measured as number of relative light units (RLU). All cell death experiments were performed after 3-4 h of infection and all IL-1β experiments were performed after 5 h of infection unless otherwise stated. Data are presented as mean ± SD of triplicate wells from three or more independent experiments. n.d. not detected. *p<0.05, **p<0.01, ***p<0.001.

Supplementary Figure 2.

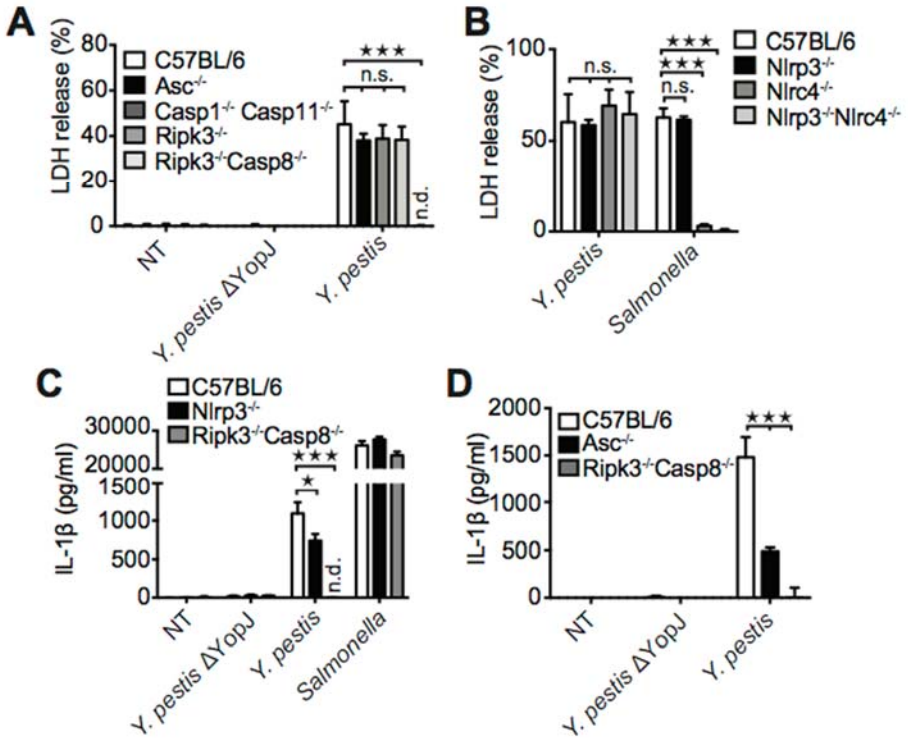

Fig. S2. Caspase-8 contributes to cell death independently of the NLRP3 inflammasome components. LDH release (**A** and **B**) and IL-1β release (**C**-**D**) was measured after 4 h (**A**, **B**) and 5 h (**C**-**D**) in the supernatants of BMDMs from the indicated genotypes after bacterial treatment Data are presented as mean ± SD of triplicate wells from three or more independent experiments. n.d. not detected. *p<0.05, **p<0.01, ***p<0.001.

Supplementary Figure 3.

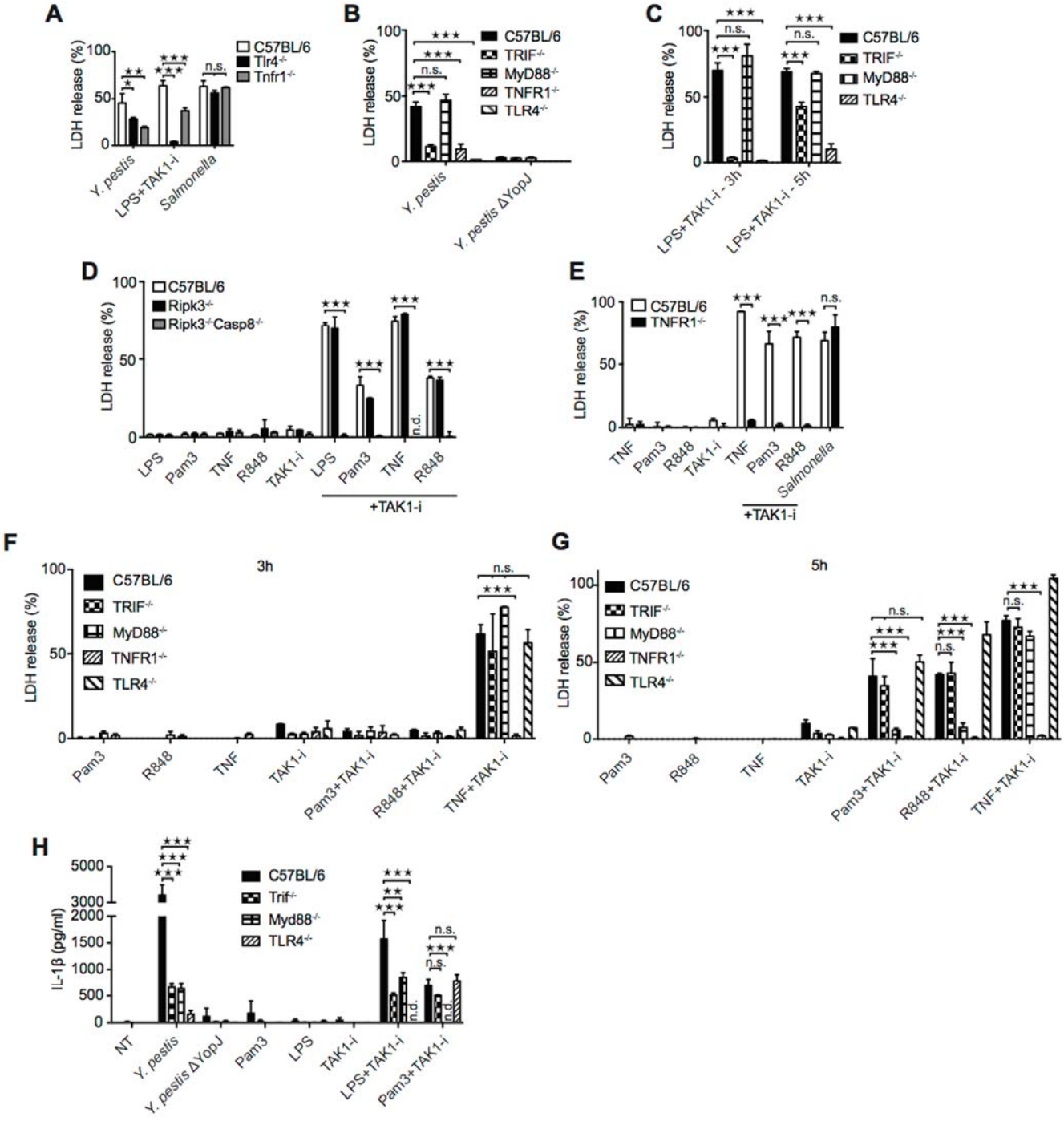

Fig S3. TRIF and TNFR1 contribute to cell death induced by infection and LPS+TAK1-i, whereas MyD88, caspase-8 and TNFR mediate cell death to TLR2 and TLR7/8 ligands plus TAK1-i at later time points. BMDM from the indicated genotypes of mice were treated for 3 h (**A, B**), 5 h (**D, E, H**) or the indicated time points with *Y. pestis*, *Salmonella*, LPS (100 ng/ml), Pam3Cys (1000 ng/ml), R848 (100 ng/ml) or TNF (50 ng/ml) in the presence or absence of TAK1-i 5z7 (400 nM). Release of LDH or IL-1β was measured. Data are presented as mean ± SD of triplicate wells from three or more independent experiments. n.d. not detected. *$p<0.05$, **$p<0.01$, ***$p<0.001$.

Supplementary Figure 4.

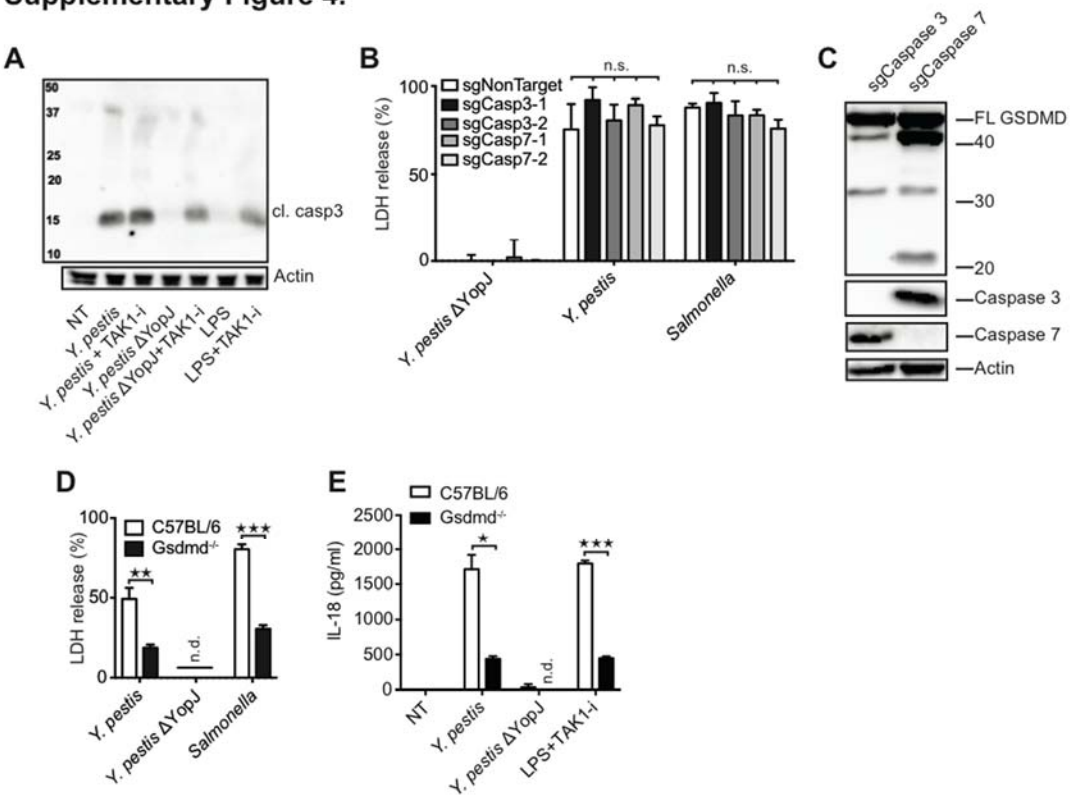

Fig. S4. Active caspase-3 cleaves GSDMD but does not contribute to cell death. (**A**) C57BL/6 BMDMs were challenged with *Y. pestis*, *Y. pestis* ΔYopJ, or LPS (100 ng/ml) in the presence or absence of TAK1 inhibition (5z7 0.4 μM), and combined cell lysates and supernatants were analyzed by immunoblot for cleaved caspase-3. (**B** and **C**) Cas9-expressing immortalized BMDMs were transduced with lentivirus containing sgRNA targeting caspase-3 or caspase-7. LDH release was measured 4 h after *Y. pestis* and *S.* Typhimurium challenge (**B**). Levels of caspase-3 and caspase-7 as well as cleaved GSDMD after challenge with *Y. pestis* were analyzed by immunoblot (**C**). (**D** and **E**) BMDMs from C57BL/6 or Gsdmd$^{-/-}$ mice were challenged with the indicated stimuli for 3 h (**D**) or 5 h (**E**) and cell death was analyzed by release of LDH (**D**) and IL-18 was analyzed by ELISA (**E**). Data are presented as mean ± SD of triplicate wells from three or more independent experiments. n.d. not detected. *p<0.05, **p<0.01, ***p<0.001.

Supplementary Figure 5.

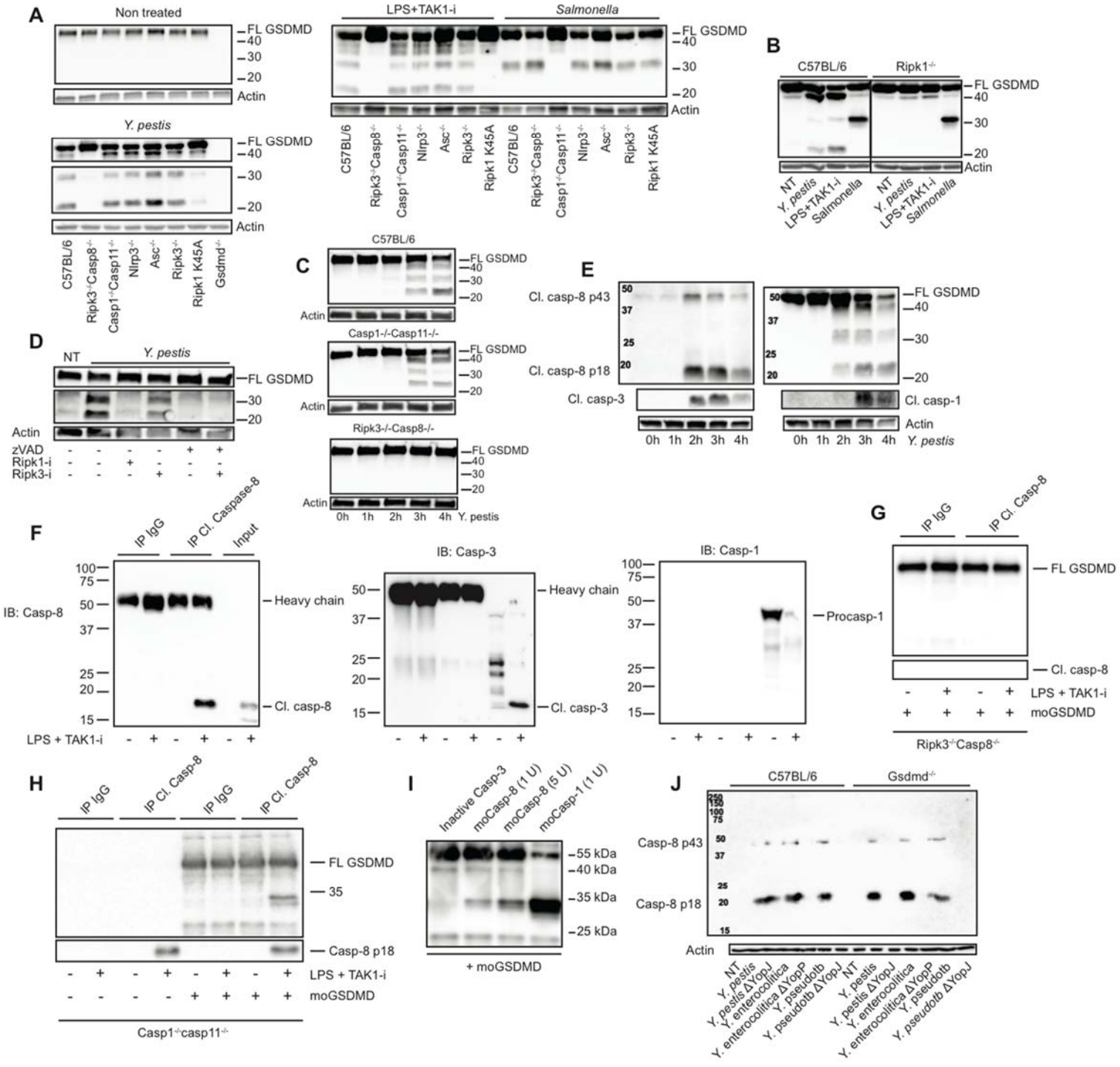

Fig. S5. TAK1 inhibition leads to cleavage of caspase-8, caspase-1, and GSDMD. (**A**) Cleaved GSDMD in untreated, *Y. pestis*, or LPS+TAK1-i (100 ng/ml LPS, 0.4 μM 5z7) and *S.* Typhimurium infected BMDMs of indicated genotypes after 3 h. (**B**) C57BL/6 or Ripk1$^{-/-}$ FLMs stimulated with *Y. pestis*, LPS+TAK1-i (100 ng/ml LPS, 0.4 μM 5z7), or *S.* Typhimurium, and analyzed for GSDMD cleavage in cell extracts after 3 h. (**C**) C57BL/6, Ripk3$^{-/-}$, and Ripk3$^{-/-}$ Casp8$^{-/-}$ BMDMs were challenged with *Y. pestis* over a 4 h time period. Cell extracts were analyzed by immunoblot for cleaved GSDMD. (**D**) C57BL/6 BMDMs were pretreated for 1 h

with the pan-caspase inhibitor zVAD-fmk (25 μM), RIPK1 inhibitor GSK'963 (1 μM), or RIPK3 inhibitor GSK'872 (3 μM) before challenged with *Y. pestis* for 3 h. (**E**) C57BL/6 BMDMs treated with Y. pestis over a time period of 4 h. Cell extracts were then analyzed by immunoblot for cleaved caspase-8, cleaved caspase-3, cleaved GSDMD and cleaved caspse-1. (**F**) C57BL/6 BMDMs were treated with LPS+TAK1-i for 3 h and then immunoprecipitated with cleaved caspase-8 antibody or IgG control antibody. Immunoprecipitated lysates were then analyzed by immunoblot for presence of cleaved caspase-8, cleaved caspase-3 or caspase-1. BMDMs from $Ripk3^{-/-}Casp8^{-/-}$ (**G**) or $Casp1^{-/-}Casp11^{-/-}$ (**H**) were treated and immunoprecipitated as in (**F**) and incubated with recombinant mouse GSDMD (2 μg) at 37°C for 1 h in a protein cleavage buffer, before being analyzed by immunoblots. (**I**) Recombinant mouse caspases (specific activity 1 U or 5 U) were incubated with recombinant mouse GSDMD as in (**G**) and (**H**) and analyzed by immunoblot. (**J**) Caspase-8 cleavage in C57BL/6 and $Gsdmd^{-/-}$ BMDMs after bacterial challenge shown by immunoblot in combined cell extracts and supernatants after 4 h. Figures are representative of three or more independent experiments.

Supplementary Figure 6.

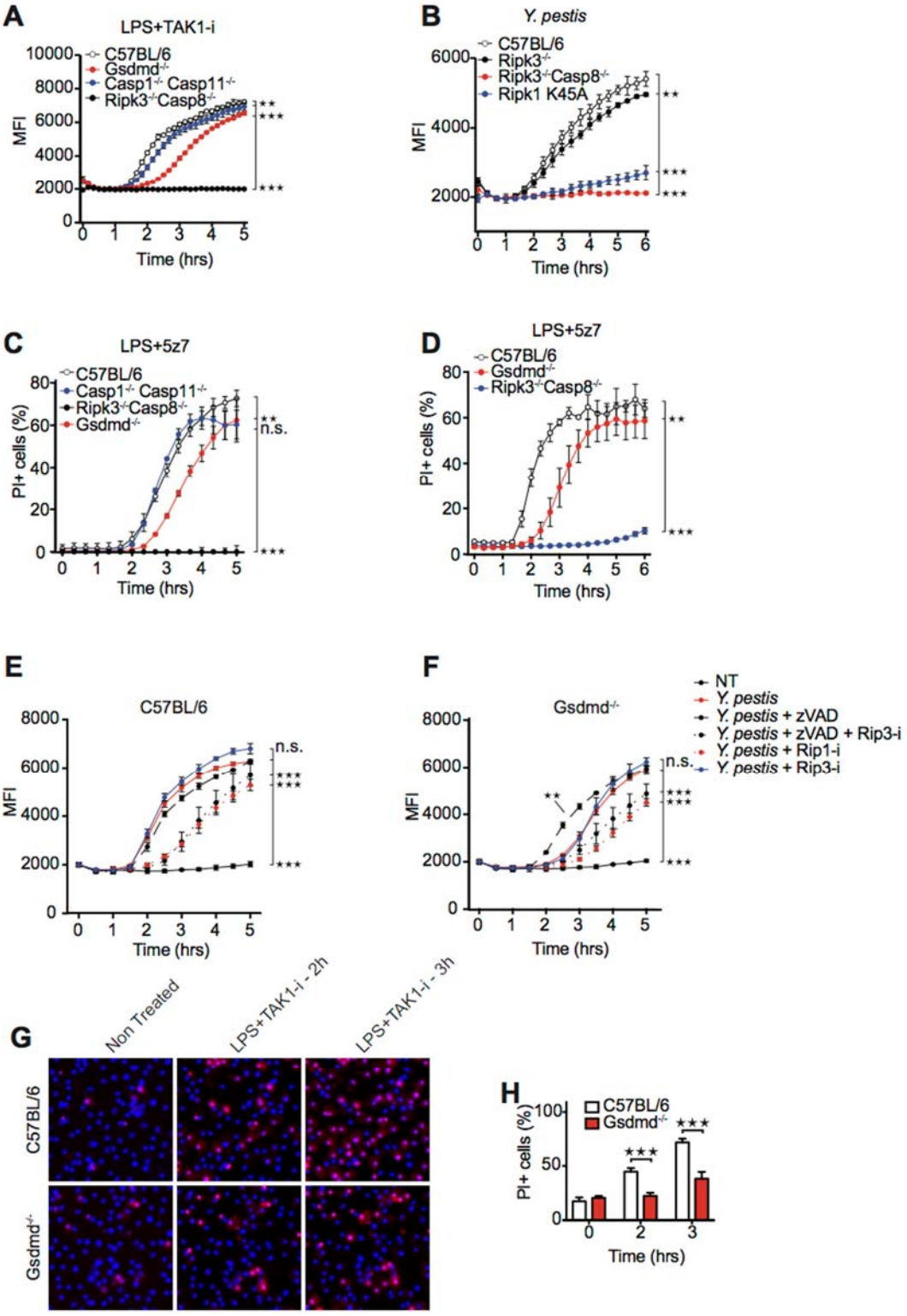

Fig. S6. Kinetic cell death measurements after TAK1 inhibition. (**A**, **B**, **E**, and **F**) Levels of DNA-bound EthD-1 (2 μM) were measured with a Synergy H4 machine (Biotek). Reads were made every 10 minutes for 5 hours (530 nm excitation, 645 nm emission) on BMDMs from the indicated genotypes treated with *Y. pestis* or LPS + TAK1-i (100 ng/ml LPS, 0.4 μM 5z7). (**C** and **D**) Cell death as measured by % PI positive cells was analyzed with a Cytation 3 machine (Biotek) with images taken every 10 minutes for 5 hours. Cells were stained with PI (1 μg/ml) and Hoescht (1 μg/ml). Gen5 software (Biotek) was used to calculate number of dead and number of total cells based on PI^+ and $Hoechst^+$ cells, after treatment with LPS + TAK1-i (100 ng/ml LPS, 0.4 μM 5z7). (**E** and **F**) C57BL/6 and $Gsdmd^{-/-}$ BMDMs were pretreated for 1 h with the pan-caspase inhibitor zVAD-fmk (25 μM), RIPK1 inhibitor GSK'963 (1 μM), or RIPK3 inhibitor GSK'872 (3 μM) before being infected with *Y. pestis*. (**G**) PI (red, 1 μg/ml) stained and Hoechst stained (blue, 1 μg/ml) cells were analyzed on a Cytation 3 (Biotek) after 2 h and 3 h of LPS + TAK-i (100 ng/ml LPS, 0.4 μM 5z7) treatment in BMDMs. (**H**) Quantification of cells in (**G**) was performed showing % PI positive cells over total Hoescht positive cells. Data are presented as mean ± SD of triplicate wells and are representative of three or more independent experiments. *$p<0.05$, **$p<0.01$, ***$p<0.001$.

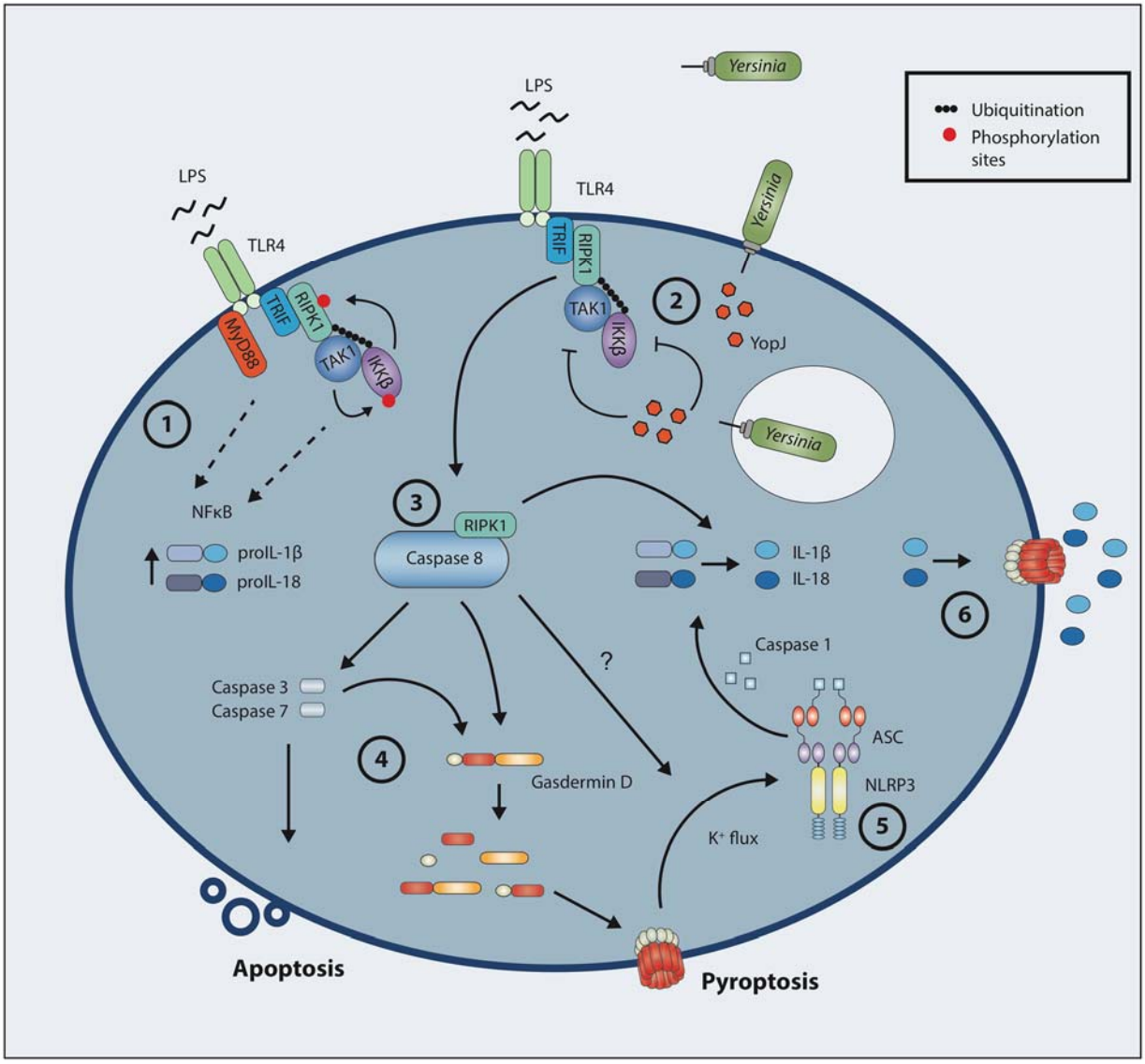

Fig. S7. Proposed model figure. 1) During infection, TLR and TNF signaling will lead to activation of NF-κB and transcription of proinflammatory genes. **2)** Secretion of the *Yersinia* effector protein YopJ leads to inhibition of TAK1 and IKK and reduced proinflammatory gene transcription. **3)** Inhibition of TAK1 and IKK triggers the activation of caspase-8 via RIPK1. **4)** Active caspase-8 cleaves and activates caspase-3 and -7 and initiates apoptosis. Simultaneously, caspase-8 also cleaves GSDMD leading to formation of GSDMD pores. **5)** GSDMD pores leads to efflux of K^+ and activation of the NLRP3 inflammasome and subsequent caspase-1 cleavage. **6)** Caspase-1, with contribution from caspase-8, cleaves pro-IL-1β and pro-IL-18, which get released through the GSDMD pores. The question mark emphasizes the fact that pore-formation and NLRP3 inflammasome still occurs in the absence of GSDMD, albeit with a 1-2 h delay, indicating that caspase-8 can directly or indirectly trigger activation of other pore-forming molecules or membrane ruptures. Secondary TNF-release together with TAK1 inhibition may also play a role in activating this pathway.

Gene	sgRNA sequence (5' – 3')
Caspase-3	CATGCAGAAAGACCATACAT
Caspase-3	CGGGGTACGGAGCTGGACTG
Caspase-7	GGACGGTTACTTCAAAACCC
Caspase-7	AACTTCGACAAAGCGACAGG

Table S1. sgRNA sequences used to knock out the indicated genes.

Figure	Genotype/condition (%)										
Fig. 1H	C57BL/6		Casp1$^{-/-}$Casp11$^{-/-}$		Ripk3$^{-/-}$		Ripk3$^{-/-}$Casp8$^{-/-}$				
	NT	*Y. pestis*	NT	*Y. pestis*	NT	*Y. pestis*	NT	*Y. pestis*			
	0	*100*	9	*150*	9	*126*	2	*0*			
Fig. 1J	C57BL/6		Nlrc4$^{-/-}$		Nlrp3$^{-/-}$		Nlrc4$^{-/-}$Nlrp3$^{-/-}$				
	NT	*Y. pestis*	NT	*Y. pestis*	NT	*Y. pestis*	NT	*Y. pestis*			
	7	100	3	0	1	88	0	0			
Fig.1K	NT	*Y. pestis*	*Y. pestis* + R1-i	*Y. pestis* + R3-i	*Y. pestis* + zVAD	*Y. pestis* + zVAD + R3-i	LZ	LZ + R1-i	LZ + R3-i	LZ + zVAD	LZ + zVAD + R3-i
	2	100	2	105	7	0	26	2	33	0	0
Fig. 2H-A	C57BL/6	Casp1$^{-/-}$Casp11$^{-/-}$	Ripk3$^{-/-}$Casp8$^{-/-}$	Gsdmd$^{-/-}$	Ripk3$^{-/-}$	MLKL$^{-/-}$	Nlrp3$^{-/-}$				
	100	90	10	29	88	98	4				
Fig. 2H-B	C57BL/6	Casp1$^{-/-}$Casp11$^{-/-}$	Ripk3$^{-/-}$Casp8$^{-/-}$	Gsdmd$^{-/-}$	Ripk3$^{-/-}$	MLKL$^{-/-}$	Nlrp3$^{-/-}$				
	100	88	6	39	109	170	3				
Fig. 2I	C57BL/6					Gsdmd$^{-/-}$					
	0h	1h	2h	3h	4h	0h	1h	2h	3h	4h	
	0	0	97	113	100	0	0	3	57	138	
Fig. 2J	NT	*Y. pestis*	*Y. pestis* + KCl	Nigericin	Nigericin + KCl						
	0	100	0	100	11						
Fig. S1J	C57BL/6			Ripk1 K45A							
	NT	*Y. pestis*	*Salmonella*	NT	*Y. pestis*	*Salmonella*					
	7	100	55	-2	-4	25					

Table S2. Quantification of western blots for ASC oligomerization assays. Band intensity was measured using ImageJ. Values were inverted and background was subtracted before being normalized to C57BL/6 *Y. pestis* infection for each experiment. For Fig. 2I, values were normalized to C57BL/6 *Y. pestis* 4 h infection. For Fig. 2J, values were normalized to *Y. pestis* or nigericin.